DALTON
FULL PAPER

Ab initio study of the protic conversion of an allene into an η^2-vinyl complex of Re, and on their structure, bonding and redox behaviour †

Maxim L. Kuznetsov,[a] Armando J. L. Pombeiro *[a] and Andrei I. Dement'ev[b]

[a] *Centro de Quimica Estrutural, Complexo I, Instituto Superior Tecnico, Av. Rovisco Pais, 1049-001 Lisboa, Portugal. E-mail: pombeiro@popsrv.ist.utl.pt*
[b] *Moscow Pedagogical State University, Chemical Department, 119021, 3 Nesvigsky per., Moscow, Russia. E-mail: chemdept@mtu-net.ru*

Received 24th May 2000, Accepted 13th September 2000
First published as an Advance Article on the web 13th November 2000

Ab initio quantum-chemical methods at the RHF/UHF and MP2 levels of theory were applied to the investigation of the structure, bonding, reactivity and electrochemical behaviour of a rhenium(I)-bis(diphosphine) η^2-allene complex and of the corresponding η^2-vinyl product derived from protonation, by using the models *trans*-[ReCl-(η^2-H_2C=C=CH_2)$(PH_3)_4$] and *trans*-[ReCl{η^2-C$(CH_2)CH_3$}$(PH_3)_4]^+$. Full geometry optimization of the models was carried out and the electrostatic potential distributions and MO compositions were calculated, allowing not only the interpretation of the co-ordination bonds of the η^2-allene and the η^2-vinyl ligands and of the relative oxidation potentials of their complexes and study of the cathodically induced dehydrogenation of the η^2-vinyl species to regenerate the parent allene complex, but also the investigation of the mechanism of protonation of the allene complex. The calculations were also performed on the possible singly and doubly protonated complexes, and the results indicate that the protic conversion of the η^2-allene into the η^2-vinyl complex conceivably occurs *via* chloro-protonated-allene and -vinyl intermediates (rather than *via* initial metal protonation), *i.e.* *trans*-[Re(ClH)-(η^2-H_2C=C=CH_2)$(PH_3)_4]^+$ and *trans*-[Re(ClH){η^2-C$(CH_2)CH_3$}$(PH_3)_4]^{2+}$, which were not identified in a previous stopped-flow spectrophotometric study, thus supporting an unprecedented role, in the protonation reaction, of the chloro-ligand which does not behave as a mere spectator or *trans*-stabilizer.

Introduction

The developments of quantum-chemical methods have allowed their application to the study of various molecular properties, with interest to experimental chemists, of many-electron systems including transition-metal co-ordination compounds.[1] Such properties include molecular structures, features of chemical bonds and their energies and, although to a lesser extent, chemical reactivity.

In particular, transition metal complexes with small unsaturated ligands, such as carbonyl,[2] carbenes, vinylidenes or carbynes,[2j,3] dinitrogen[2n,4] or π-bonded ligands,[3e,l,5] have been the object of various theoretical studies, which have also been applied, although scantily, to η^2-allene or η^2-vinyl (or η^2-allenyl) complexes.[3m,6] Examples of their reactions investigated by theoretical methods include insertions of olefins, acetylenes or carbonyl, hydrogen-transfer reactions,[1a] hydrogenation of CO, CO_2 and olefins, hydroformylation of olefins,[1c] electrophilic or nucleophilic addition to carbynes, carbenes, acetylide, vinylidene, vinyl and isocyanide ligands,[2j,3c,h–k,7] the Dötz reaction,[1c] catalytic dimerization of ethylene and polymerization of allene[6c] and acetylene-to-vinylidene rearrangement.[3l,8]

However, applications of quantum-chemical methods to the elucidation of the *mechanisms* of reactions of organometallic complexes have less extensively been reported,[1a,c,3l,9] and in this study we present our attempts to complement, by *ab initio* methods, a mechanistic investigation by stopped-flow spectrophotometry[10] of protonation of the η^2-allene complex *trans*-[ReCl(η^2-H_2C=C=CHPh)$(dppe)_2$] **1** (dppe = $Ph_2PCH_2CH_2PPh_2$) to give the η^2-vinyl *trans*-[ReCl{η^2-C$(CH_2)CH_2Ph$}$(dppe)_2]^+$. This reaction, which then constituted a novel method for the synthesis of η^2-vinyl complexes,[6b] is based on an electrophilic rather than on a nucleophilic addition, and its complex rate law is not consistent with direct protonation at the phenyl-substituted carbon atom, but instead with a mechanism (Scheme 1) involving an initial protonation at a different site,

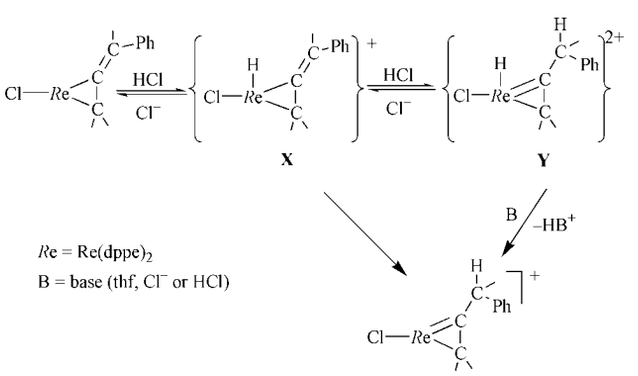

Scheme 1 Mechanism of protonation of the allene complex *trans*-[ReCl(η^2-H_2C=C=CHPh)$(dppe)_2$] proposed[10] on the basis of a stopped-flow spectrophotometric study. **X** and **Y** were postulated intermediates.

followed by intramolecular and acid–base catalysed rearrangements.

The initial site of protonation was not ascertained, but the metal was simply *postulated* as such a site, apparently consistent with preliminary extended Hückel calculations (performed on a model system with the ligated allene CH_2=C=CH_2 and with all

† Electronic supplementary information (ESI) available: molecular orbital diagrams of complexes **2** and **4**. See http://www.rsc.org/suppdata/dt/b0/b004143m/

the other ligands taken as hydrogens)[6b] which indicate that the HOMO of the complex is predominantly metal-based. The mono- and the di-protonated intermediates **X** and **Y** were not identified and the kinetic analysis would fit any formulations presenting any other atom (apart from the phenyl-carbon atom) as the initial site of proton attack. In view of the relevance of the elucidation of this point, we have performed more extensive *ab initio* studies on a more elaborate model system (see below), aiming to be able to select the most probable site for the initial H^+ addition and to identify the key intermediate complexes **X** and **Y**.

Other aims of this study include the understanding of the co-ordination bonds of the ligated allene and η^2-vinyl, as well as of the redox properties and electrochemical behaviour[11] of their complexes.

Computational details

The full geometry optimization of model fragments in Cartesian coordinates and the calculation of molecular orbital composition for compounds with a closed electron shell were carried out by the quasi-Newton–Raphson gradient method at the restricted Hartree–Fock approximation using effective core potentials (ECPs)[12] with help of the GAMESS package.[13] The relative energies of all structures include zero-point energy (ZPE) correction. The calculations of the molecular orbital composition of fragments with an open electron shell were carried out by the unrestricted Hartree–Fock method. Vertical ionization potentials of the initial allene and final vinyl complexes were calculated at both HF and MP2[14] levels of theory. Symmetry operations were not applied for all structures. A quasi-relativistic Stuttgart pseudopotential described 60 core electrons and the appropriate contracted basis set (8s7p6d)/[6s5p3d][15] for the rhenium atom were used. For other non-hydrogen atoms the analogous pseudopotentials and basis sets[16] were applied. The standard basis set of Gauss functions 6-31G[17] was selected for the hydrogen atoms.

The electrostatic potential values for the starting allene complex were determined for the grid of points in the plane of the allene fragment and in the parallel planes (at distances of 1, 2 and 3 Å from the plane of the allene fragment) with step points of 0.1 Å. The Hessian matrix was calculated numerically for all structures in order to prove the location of correct minima (for the initial and all mono- and di-protonated structures there are no imaginary frequencies) or saddle points (for transition states there is only one negative eigenvalue).

The hypothetical complex *trans*-[ReCl(η^2-CH_2=C=CH_2)-(PH_3)$_4$] **2** instead of the real one *trans*-[ReCl(η^2-CH_2=C=CHPh)-(dppe)$_2$] **1** was chosen as a model compound for our calculations. The choice of the basis set and of the model took into account a reasonable computational time required for geometry optimization. Figures with MO diagrams for **2** and for the reduced form **4′** of the derived η^2-vinyl complex **4** have been deposited as Electronic Supplementary Information (ESI).

Results and discussion

Structure of the allene complex *trans*-[ReCl(η^2-CH_2=C=CH_2)-(PH_3)$_4$] 2

The equilibrium structure (**2**, Fig. 1), which was found as a result of the full geometry optimization of *trans*-[ReCl-(η^2-CH_2=C=CH_2)(PH_3)$_4$], represents a slightly distorted octahedron (if the allene ligand is considered to occupy a single co-ordination position). The relative positions of the allene and the {ReCl(PH_3)$_4$} fragment correspond to the eclipsed conformation exhibited by the real complex **1**:[18] two, P(10) and P(11), of the P atoms (as well as the Cl(13) atom) lie in the plane of the allene carbon-framework and are shifted away from the allene ligand due to steric effects, the P(10)ReP(11) angle of 160.6° being significantly smaller than that (179.1°) of P(9)ReP(12).

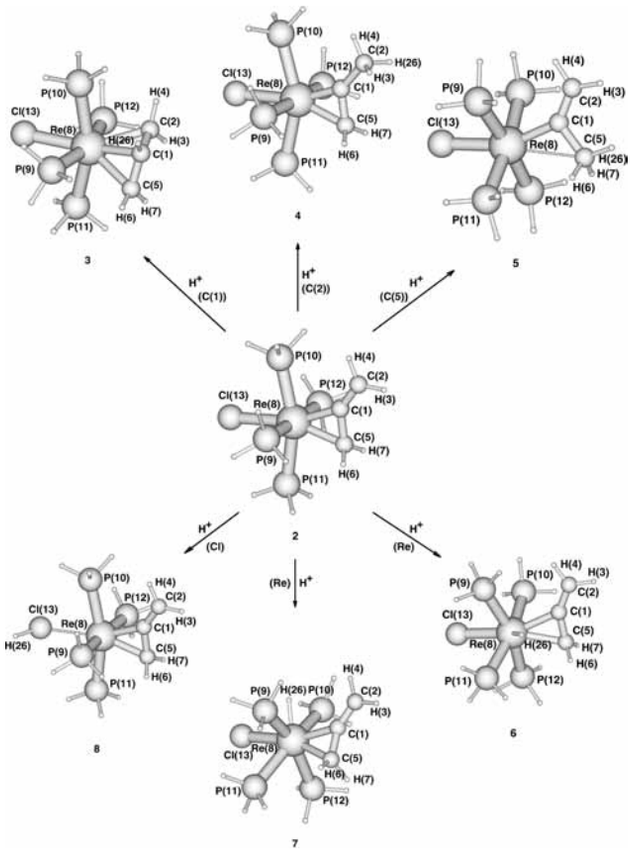

Fig. 1 Optimized structures for the allene complex **2** and for the derived monoprotonated complexes **3**–**8** (numbers following the order of increasing energy) (**8** is the most favourable intermediate towards **4**).

Selected bond lengths and angles are given in Table 1 and the main calculated structural parameters are in agreement with the experimental ones measured for complex **1**. In particular, the calculated C(1)–C(2) and C(1)–C(5) bond lengths, 1.325 and 1.421 Å, are close to the respective measured values, 1.32(1) and 1.41(1) Å.[18] The former corresponds to a double bond (bond order of 1.89) and the latter is rather extended by co-ordination (the C=C distance in the free allene molecule calculated at the same approach is 1.299 Å) becoming *ca.* 0.08–0.09 Å shorter than the average C–C single bond distance.[19] The Re–C(1) bond length (2.110 Å) is shorter than Re–C(5) (2.199 Å), and these features are in accord with both X-ray data (2.087(6) and 2.181(6) Å, respectively[18]) and results of preliminary quantum chemical calculations by the extended Hückel method on a simpler model of **1**.[6b]

Monoprotonated structures

One of the aims of this work is the recognition of centres susceptible to protonation and the search for possible protonated structures. The effective atomic charges (Table 2) provide preliminary information on this subject. The highest negative value is localized at the chloro atom Cl(13) (−0.59), followed by the C(2) and C(5) atoms (−0.42 and –0.41, respectively), whereas less negative values were obtained for the Re and C(1) atoms.

In order to determine the most probable ways of H^+ approaching for protonation of the allene structure **2**, the electrostatic potential (ESP) distribution was calculated and is illustrated (Fig. 2) by the maps of negative ESP for the plane in which the allene fragment lies (z = 0 Å) and for the parallel plane at 1 Å distance (z = 1 Å). The negative ESP values are distributed according to two main conical shapes and several regions with the highest negative ones can be distinguished. The ESP is

Table 1 Selected bond lengths (Å) and angles (°) for structure **2** and derived mono- and di-protonated ones

	2	**3**	**4**	**5**	**6**	**7**	**8**	**9**	**10**	**11**	**12**
C(1)–C(2)	1.325	1.399	1.476	1.324	1.309	1.313	1.319	1.472	1.487	1.465	1.488
C(1)–C(5)	1.421	1.399	1.423	1.527	1.375	1.384	1.403	1.411	1.518	1.404	1.360
Re–C(1)	2.110	2.292	1.935	2.072	2.254	2.177	2.131	1.948	1.965	1.991	2.933
Re–C(5)	2.199	2.336	2.175	2.690	2.316	2.262	2.220	2.174	2.876	2.197	2.498
Re–C(2)		2.336									
Re–P(av.)	2.52	2.57	2.56	2.58	2.56	2.58	2.54	2.58	2.60	2.60	2.61
Re–Cl(13)	2.644	2.563	2.570	2.511	2.570	2.574	2.963	3.106	2.454	2.522	2.381
Re–H					1.631	1.645				1.636	
Cl(13)–H							1.309	1.311			
C(2)–C(1)–C(5)	138.4	116.2	131.3	122.2	148.7	145.5	140.8	133.3	114.1	134.9	125.7
Re–C(5)–C(1)	67.4	70.7	60.9	50.1	70.0	68.5	67.8	61.6	39.7	62.7	94.3
Re–C(1)–C(5)	74.2	74.2	79.1	95.5	75.0	75.2	74.6	78.9	110.7	78.6	58.2
C(2)–C(1)–Re	147.4	74.1	149.6	142.3	136.3	139.2	144.6	147.8	135.2	146.5	114.1
C(1)–Re–P(9)	89.9	88.9	95.0	79.7	89.8	90.0	85.5	93.3	86.4	88.2	78.5
C(1)–Re–P(10)	81.7	88.8	83.4	79.7	76.4	87.2	81.7	84.9	86.4	93.6	87.8
C(1)–Re–P(11)	117.8	111.2	117.7	110.9	122.6	121.0	115.8	117.4	105.5	96.3	93.5
C(1)–Re–P(12)	90.8	111.2	95.1	110.9	108.5	93.8	88.8	92.9	105.2	121.9	110.8
H–Re–C(1)					62.8	77.6				81.8	
H–Re–C(5)					70.9	107.8				112.7	
H–Re–Cl(13)					130.0	86.4				82.6	
H–Re–P(9)					71.3	60.6				61.7	
H–Re–P(11)					65.3	137.9				139.8	
H–Cl(13)–Re							118.0	132.6			

Table 2 Mulliken atomic charges for the initial and protonated structures

	Charge						
Atom	**2**	**3**	**4**	**5**	**6**	**7**	**8**
C(1)	−0.12	−0.13	−0.15	−0.26	−0.10	−0.08	−0.13
C(2)	−0.42	−0.44	−0.46	−0.43	−0.38	−0.37	−0.39
C(5)	−0.41	−0.44	−0.47	−0.54	−0.26	−0.33	−0.37
Re(8)	−0.30	−0.48	−0.30	−0.17	−0.70	−0.62	−0.42
P(9)	0.39	0.42	0.42	0.46	0.45	0.51	0.40
P(10)	0.41	0.42	0.42	0.46	0.44	0.48	0.41
P(11)	0.42	0.45	0.45	0.39	0.47	0.39	0.41
P(12)	0.38	0.45	0.42	0.39	0.44	0.42	0.37
Cl(13)	−0.59	−0.45	−0.45	−0.41	−0.44	−0.45	−0.18

minimum in the neighbourhood of the chloro-atom, Cl(13) (**I**, Fig. 2) and the following regions include the minima near the C(2), C(5) and C(1) atoms (**II**–**VI**). Finally, there are only a few points (**VII**) with negative ESP between the Re and the C(5) atoms. Since the chloro-atom, the C(5) and C(2) atoms have the highest negative atomic charge and taking also into account that the regions with the most negative ESP are situated near these atoms, they constitute the most probable centres for protonation according to the simple electrostatic model. In contrast, the proton attack on the Re atom appears rather unlikely.

In order to establish the possibility of formation of the different protonated structures and to estimate their relative stability, full geometry optimization of the series of protonated structures with different starting positions of the attacking proton (initially placed in the regions with the most negative ESP) was carried out. The minima on the potential surface were found for all the following possible monoprotonated structures ordered according to the decrease of their stability (Table 3). The most stable one (**3**, Fig. 1) is that with the protonated C(1) atom, thus presenting an η^3-allyl ligand, η^3-CH_2CHCH_2, formed when the proton approaches that atom from the region over or under the plane of the allene fragment. The formation of this η^3 structure leads to analogous distances between Re and all the carbon atoms, *i.e.* the Re–C(1), Re–C(2) and Re–C(5) bond lengths are 2.292, 2.336 and 2.336 Å (Table 1) and the existence of a π-delocalized bond is confirmed by the similar values of the effective Mulliken atomic charges on the C(2) and C(5) atoms (−0.44), and by the identical C(1)–C(2) and C(1)–C(5) bond lengths (1.399 Å) and orders (1.13). The

Table 3 Total energies of the initial and protonated structures E_{tot}, relative energies E_{rel} and zero point energies (ZPEs)

Structure	Protonated atom	E_{tot}/ Hartree	E_{rel}/ kcal mol^{-1}	ZPE/ kcal mol^{-1}
2	—	−143.33967	0.0	112.3
3	C(1)	−143.75944	0.0	122.5
4	C(2)	−143.74348	+9.9	120.4
5	C(5)	−143.73124	+17.5	120.4
6	Re	−143.69820	+38.5	119.9
7	Re	−143.68151	+48.9	119.9
8	Cl(13)	−143.66576	+58.8	117.4
9	Cl(13), C(2)	−143.93637	+29.3	124.8
10	C(5), C(2)	−143.98288	0.0	128.2
11	Re, C(2)	−143.91540	+42.4	128.0
12	C(1), C(2)	−143.98036	+1.6	128.7

Re–P bond elongates (to 2.560–2.578 Å) while the Re–Cl(13) distance shortens (to 2.563 Å) and these features are common to all the other protonated structures discussed below, with the exception of the one that results from protonation at the chloro-ligand. They are accounted for by the decrease of the π-electron release ability of Re to the phosphines and the enhancement of the π-electron donation of the chloro-ligand, as a result of the protonation of the allene.

The second most stable protonated structure (**4**, Fig. 1), whose total energy is 9.9 kcal mol^{-1} higher than that of **3**, is formed when the proton approaches the molecule from the C(2) atom side, and corresponds to the final η^2-vinyl product of the

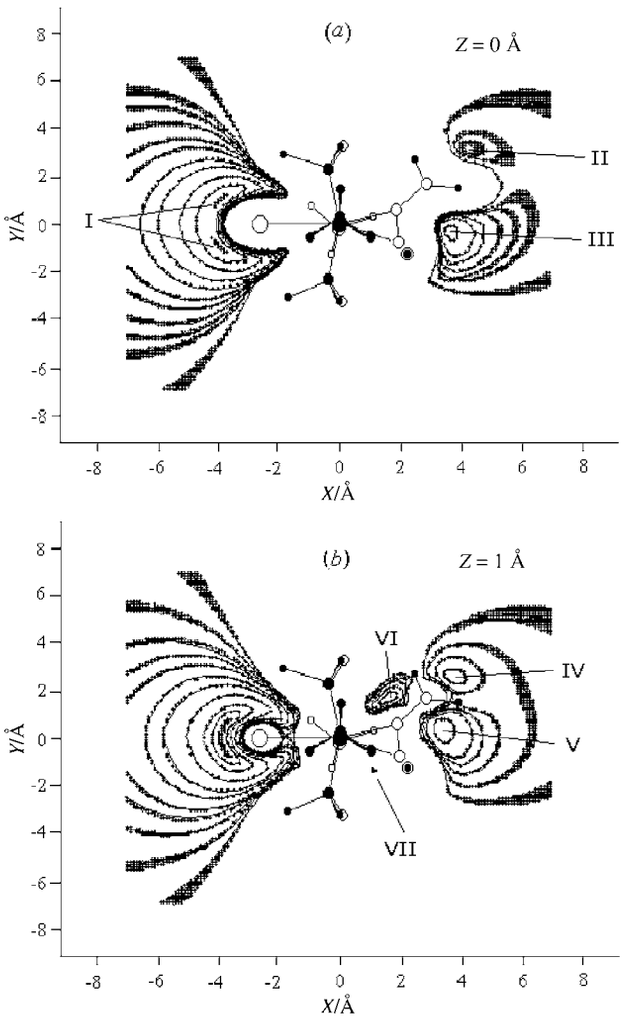

Fig. 2 Distribution of electrostatic potential for compound **2**: (a) in the plane of the allene fragment ($z = 0$ Å); (b) in the parallel plane at 1 Å distance ($z = 1$ Å).

protonation of complex **1**.[6b,10] Structure **4** presents a plane of symmetry with the Cl, Re, C and two of the P atoms, the other two being symmetrically located on each side of this plane. Protonation of the initial complex at C(2) leads to a shortening of the Re–C(1) bond length to 1.935 Å and an elongation of the C(1)–C(2) distance to 1.476 Å (Table 1), *i.e.* to a single bond length (the bond order is 0.91). The C(1)–C(5) distance remains virtually unchanged and the Re–Cl(13) and Re–C(5) bonds are shortened to 2.570 and 2.175 Å, respectively. The structural changes are generally in good agreement with the X-ray data[6b] which show *e.g.* that the final η^2-vinyl complex *trans*-[ReCl{η^2-C(CH_2)CH_2Ph}($dppe)_2$][BF_4] exhibits Re–C(1) and C(1)–C(2) bond lengths of 1.947(6) and 1.500(8) Å, respectively.

Geometry optimization of the protonated complexes with the initial proton position near the C(5) atom leads to structure **5** (Fig. 1) with this protonated atom (forming an η^1-vinyl species), whose total energy is 7.6 kcal mol^{-1} higher than that of **4**. It is noteworthy that, for the initial H^+ position between the Re and C(5) atoms (**VII**, Fig. 2), the proton moves not to the metal but to the latter atom. This protonation is accompanied by a change of the general molecular conformation, *i.e.* the organic ligand in an eclipsed position relative to two of the P atoms, in **2**, becomes situated between PH_3 ligands in **5**. A minimum corresponding to the eclipsed conformation of allene and PH_3 ligands was not found.

Structure **5** also has a symmetry plane containing the Re, Cl(13) and C atoms. As a result of protonation a strong weakening (conceivably leading to cleavage for the real system) of the Re–C(5) bond occurs [this interatomic distance becomes 2.690 Å (Table 1)] with formation of the η^1-vinyl complex, consistent also with elongation of the C(1)–C(5) bond (to 1.527 Å) without significant variation of the C(1)–C(2) distance.

The next structure in the order of stability (**6**, Fig. 1, 21.0 kcal mol^{-1} less stable than **5**) results from protonation at the metal and its formation requires overcoming a potential barrier. The initial proton position within any region with negative ESP (including regions **VI** and **VII**, Fig. 2) leads to protonation of an atom different from Re. The co-ordination polyhedron of the hydride species **6** is a capped octahedron with increased Re–C(1), Re–C(5) and Re–P bond lengths to 2.254, 2.316 and 2.536–3.590 Å, whereas the C(1)–C(2), C(1)–C(5) and Re–Cl(13) bond distances are shortened to 1.309, 1.375 and 2.570 Å, respectively (Table 1).

The formation of another Re-protonated structure (**7**, Fig. 1), which is 10.4 kcal mol^{-1} less stable than **6**, would also need to overcome a potential barrier and cannot be obtained by geometry optimization with the initial H^+ position within any region with negative ESP. The proton adds to Re pushing two of the PH_3 groups [P(9) and P(10), with increasing P(9)ReP(10) angle to 122.3°] and the co-ordinational polyhedron of structure **7** is a pentagonal bipyramid with the base defined by the Re, four P atoms and the hydride ligand, with the torsion angles PPPP and P(12)P(11)P(9)H(26) 25.9 and −25.6°, and the apical sites being occupied by the Cl(13) atom and the middle point of the C(1)–C(5) bond. The C–C, Re–H and Re–Cl(13) bond lengths are similar to those of structure **6** whereas the Re–C bonds are shorter for **7** (Table 1).

The next equilibrium structure **8** (Fig. 1) exhibits a protonated chloroatom, is formed when the proton approaches molecule **2** from the side of the ligating chloride, and has the least stability (9.9 kcal mol^{-1} less stable than **7**). This protonation leads to a lengthening of the Re–Cl(13) bond to 2.963 Å (Table 1) which corresponds to rather pronounced weakening or even cleavage of this bond. The other structural parameters only undergo slight adjustments and the basic structure is virtually preserved. Hence, *e.g.* the other metal–ligand bonds extend slightly (by *ca.* 0.02 Å) in accord with a decrease of the π-electron release ability of the metal on conversion of the strong electron-donor chloride ligand into the weakly bound HCl.

Mechanism of protonation

According to stopped-flow spectrophotometric results,[10] the first stage of the protonation reaction of the allene complex involves proton addition to an atom different from C(2) giving an unidentified monoprotonated intermediate. The above theoretical study identified five such intermediates derived from protonation at C(1) (**3**), C(5) (**5**), Re (**6** and **7**) or Cl(13) (**8**). Let us now discuss their feasibility in terms of mechanistic significance.

First protonation step. The chloro-ligand in the allene complex **2** should constitute the most probable site of proton attack (forming species **8**) if the reaction is charge controlled. In fact, the most negative value (−0.59) of the effective Mulliken atomic charge in the allene complex is localized at the chlorine atom, Cl(13), and the largest regions with the most negative ESP are close to this atom.

Moreover, in comparison with the other monoprotonated equilibrium structures, **8** is that which requires the smallest structural changes relative to its parent allene complex and corresponds to the least steric hindrance to the H^+ approach to the molecule of the latter compound. The extent of the required structural rearrangements on the first protonation is a feature to consider for selection of the most probable singly protonated product since its formation is fast, occurring quantitatively during the deadtime (2 ms) of the stopped-flow spectrophotometer. In accord with this requirement, the structural arrangement

resulting from protonation of the Cl(13) atom corresponds mainly to a labilization of its bond to the metal. This effect could account for the known[20] replacement of the chloro- by a fluoro-ligand in the related protonation reaction, by HBF_4, of the vinylidene complexes *trans*-[ReCl(=C=CHR)(dppe)$_2$] (R = alkyl or aryl) to form the fluoro-carbynes *trans*-[ReF(≡CCH$_2$R)(dppe)$_2$][BF_4] together with the corresponding chloro-products.

In addition (see below), a p orbital of the chloro-ligand provides a noticeable contribution (7.9%) to the HOMO of the initial allene complex, which could be favourable in terms of a frontier-orbital argument (although not so much as for the metal atom which provides the greatest contribution to the HOMO).

The C(2) and C(5) atoms of the allene species constitute the next centres (following the chloro-ligand) with the most negative effective atomic charge (−0.42 and −0.41, respectively). Extensive regions of negative ESP are found close to the C(2), C(1) and C(5) atoms, but for all of them the ESP is much less negative than that for the more extensive one close to the chloro-ligand. The H^+ approach to the C(2) or C(5) atoms in the real phenylallene-bis(dppe) complex would be expected to be subject to a significant steric hindrance imposed by the phenyl rings of the phenylallene or of the phosphine ligands [the bulkiness of a metal bis(dppe) site is well known[21]]. Those features hamper protonation at either C(2) or C(5), at least relatively to the chloro-ligand, and conceivably also account for the non-occurrence, as shown[10] by stopped flow, of the first proton attack at C(2) which would lead directly to the final η^2-vinyl product **4**.

Further unfavourable arguments for the initial proton attack at C(5) can be put forward, in particular the significant structural alterations that would occur with formation of the η^1-vinyl ligand (complex **5**) involving *e.g.* strong weakening (or cleavage) of the Re–C(5) bond and a change of conformation. Moreover, in contrast to C(2) and Cl(13), the C(5) atomic orbitals give no contribution to the HOMO of the starting allene complex (see below) and therefore, also from the frontier-orbital point of view, the first proton addition to C(5) would not be so favourable as protonation at the chloro-ligand or even at the C(2) atom. Hence, since the initial protonation does not occur at C(2),[10] we believe the same should happen for the less favourable C(5) atom, thus ruling out complex **5** as the monoprotonated intermediate.

Rhenium is the next atom, following Cl(13), C(2) and C(5), with the most negative effective atomic charge (−0.30) and its protonation would lead to formation of the hydride complexes **6** or **7**. However, no extensive region of negative ESP was found near the Re atom and the hydride structures would be formed only when the proton is initially situated near that atom in a region with positive ESP. The geometry optimization of the structures with initial H^+ positions within the negative ESP regions leads to the formation of other protonated structures. The increase of co-ordination number of a rather sterically crowded metal centre and the steric hindrance to the H^+ approach to the metal constitute further difficulties to overcome. In this respect, we should mention that we never obtained, in our extensive protonation studies of *trans*-[ReCl(L)(dppe)$_2$] (L = CNR, NCR, alkyne, or any derivative), any hydride complexes of the type [ReH(Cl)(L′)(dppe)$_2$]$^+$ (L′ = L or derivative). Finally, the formation of hydride structures is accompanied by significant structural changes. Nevertheless, Re is the atom that mostly contributes to the HOMO (the Mulliken atomic population at Re is 1.32) (see below) and its protonation would be the most favourable one, if frontier-orbital controlled.

The next atom in the order of decreasing negative effective atomic charge is C(1) and its protonation would lead to the η^3-allyl complex **3** which corresponds to the most stable monoprotonated structure, being even more stable than the final η^2-vinyl product **4**. Therefore, its involvement in the formation of **4** should be neglected. This can be accounted for by the following factors, apart from the small negative effective charge (−0.12) at C(1): extensive structural rearrangements required and hampered sterically, especially for the real system containing nine phenyl groups, namely rotation of the organic ligand with conversion into a trihapto one leading to unacceptable eight-co-ordination of a rather bulky metal centre; strong steric hindrance to the approach of H^+ towards C(1); small contribution of this atom to the HOMO (Mulliken atomic population of 0.08, see below).

From the above considerations, the most probable site for the first proton attack at the allene complex appears to be the chloro-ligand, forming the monoprotonated intermediate **8**, thus following a charge controlled process. We now analyse the possibility of conversion of this species (or even of another less probable intermediate) into the final η^2-vinyl product **4**.

Acid–base catalysed path. The second stage of the protonation reaction can follow[10] an acid-independent pathway or an acid–base catalysed one (Scheme 1), the former occurring *via* intramolecular proton migration to the C(2) atom and the latter involving a second proton addition which occurs at this atom followed by elimination of the first proton. The acid catalysed pathway should be predominant[10] under the experimental conditions used, in the presence of an excess of acid, and will be the first one to be considered.

The monoprotonated complex with the most probable formation (see above), *i.e.* the chloro-protonated species (**8**), can account for the formation of the doubly protonated intermediate in the acid–base catalysed path, by undergoing a second proton addition to the C(2) carbon to form the diprotonated η^2-vinyl species **9** [Scheme 2(a)]. The negative

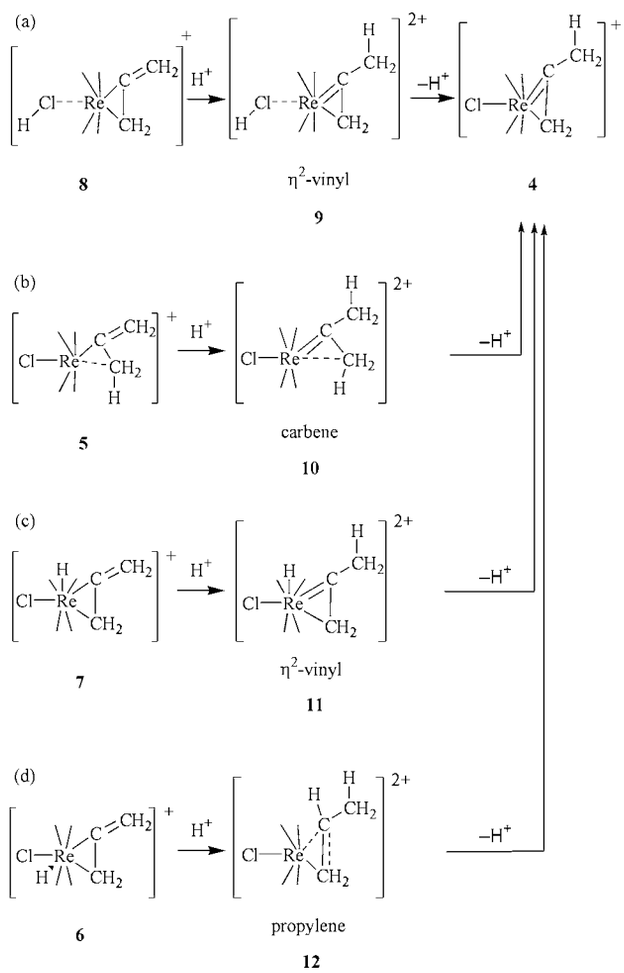

Scheme 2 Acid–base catalysed pathways [(a) as the most favourable one].

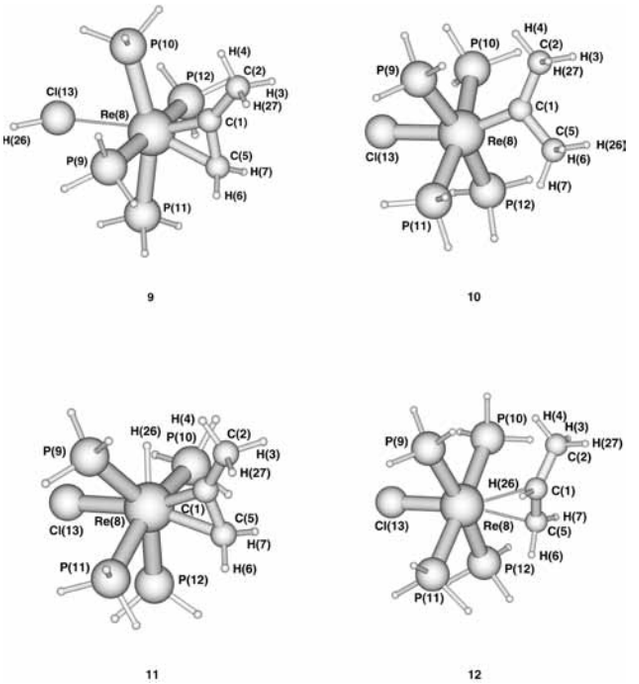

Fig. 3 Optimized structures for the hypothetical diprotonated intermediates in the acid–base catalysed pathway (**9** is the most favourable one).

value (−0.39) of the Mulliken atomic charge at the C(2) atom in **8** and its high atomic orbital contribution to the HOMO (Mulliken atomic population of 0.46) constitute favourable features for the occurrence of protonation at this particular atom. Moreover, although there are no regions of negative ESP for **8** due to the overall positive charge of the complex (nevertheless the situation can be different for the real system in which the positive charge is compensated by that of the counter ion), the least positive ESP (for the plane with $z = 2$ Å) is localized over the C(2) atom, thus constituting a further favourable condition for protonation at C(2). The preference, for the H^+, of this C atom in **8**, relatively to the other atoms, in spite of the similarity of the negative Mulliken atomic charge values for C(5) (−0.37) and Re (−0.42) [at C(1) or at Cl(13), the value, −0.13 or −0.18, respectively, is not so negative], can further be accounted for by the smallest structural changes and the least steric hindrance [in comparison with the metal and with C(1)] associated with the H^+ addition to C(2).

Full geometry optimization of the doubly protonated structure **9** (Fig. 3) was carried out on the basis of the equilibrium geometry of structure **8** as the initial one, and considering the initial position of the second proton close to the C(2) atom. The addition of the second proton to C(2) resulted in a C(1)–C(2) bond length increase to 1.472 Å (decrease of the bond order from 1.91, in **8**, to 0.90) and in a shortening of the Re–C(1) distance to 1.948 Å (Table 1), reflecting the conversion of the η^2-allene into the η^2-vinyl ligand. The other structural parameters do not change considerably.

An increase of the acidity of the HCl ligand is expected to result from protonation of the allene in species **8** to afford the dicationic complex **9** and therefore deprotonation in the latter can occur by any base present such as the solvent (thf), Cl^- or even HCl (a weak acid in this solvent).The acid–base catalysed pathway is thus completed giving the final η^2-vinyl product **4** [Scheme 2(a)].

The other diprotonated intermediates **10**–**12** that could be considered in this pathway are shown in Scheme 2(b)–(d) with their parent monoprotonated species and their geometry optimization was also achieved. They are less favourable than **9** because their parent complexes are less favourable than that of the latter, and also due to some particular reasons given below.

In the case of the C(5)-monoprotonated complex **5**, proton addition to C(2) would give the dimethylcarbene complex **10** [Scheme 2(b)] which on deprotonation of the C(5)–Me group would form the final η^2-vinyl product **4**. Relative to the parent complex **5**, the Re–C(1) bond length shortens to 1.965 Å (Table 1), thus reflecting the carbene character of the new ligand, whereas the Re–C(5) distance is stretched to 2.876 Å, corresponding to further weakening or even cleavage of the bond. The C(1)–C(2) bond length increases to 1.487 Å (conversion from double into single bond) and the C(2)C(1)C(5) angle decreases from 122.2 to 114.1°. A shortening of the Re–Cl(13) bond occurs (to 2.454 Å), as observed for the other doubly protonated structures discussed below. Complex **10** would be the most stable diprotonated species and conceivably the least acidic one, a feature that would disfavour the following deprotonation step.

The structure with both Re and C(2) protonated atoms, **11**, obtained [Scheme 2(c)] on the basis of the parent pentagonal bipyramid structure **7** is stable (in contrast with that, see below, derived from the capped octahedral hydride complex **6**), although its total energy is higher than those of the other doubly protonated structures (Table 3). The co-ordination polyhedron (Fig. 3) remains a pentagonal bipyramid, the Re–C(5) and Re–C(1) bonds are shortened to 2.197 and 1.991 Å, respectively, whereas the C(1)–C(2) bond length increases (by 0.152 Å) to 1.465 Å (Table 1), a value similar to the corresponding one in the product **4** (decrease of the bond order from 1.93 in **7** to 0.92 in **11**). The Re–Cl(13) bond length decreases to 2.522 Å while the Re–H(26) distance does not change significantly.

The structure with both Re and C(2) protonated atoms obtained [Scheme 2(d)] on the basis of the hydride precursor structure **6** (capped octahedron) is unstable. By geometry optimization, migration of the proton from the metal to the C(1) atom is observed, resulting in structure **12** (Fig. 3) with protonated C(1) and C(2) atoms giving a propylene ligand. The formation of **12** involves a twist of the organic ligand by *ca.* 90° around the C(1)–C(5) bond, the lengthening of the C(1)–C(2) bond to 1.488 Å (Table 1) (the bond order becomes 0.94), extensive weakening or even cleavage of the Re–C(1) bond [the Re–C(1) distance becomes 2.933 Å, Table 1] and elongation of the Re–C(5) bond from 2.316 to 2.498 Å. This would correspond to an effective labilization of the propylene ligand. In this respect, it is worth mentioning that we always failed in our attempts to bind an olefin to the {ReCl(dppe)} site. Hence, the corresponding pathway to the η^2-vinyl product does not appear to be favourable.

In summary, the acid–base catalysed pathway conceivably proceeds according to Scheme 2(a), *via* intermediates **8** and **9**, on the basis of the following arguments: (i) these complexes are the most favourable monoprotonated and doubly protonated intermediates, respectively, on the basis of combined favourable Mulliken atomic charges, ESP distribution, steric, structural and frontier-orbital arguments; (ii) moreover, other possible (but less favourable than **8**) monoprotonated intermediates (**5** and **6**) would lead to unfavourable diprotonated species, **10** and **12** [Scheme 2(b) and 2(d)] on account of the expected low acidity or lability of their organic ligands (carbene or propylene, respectively). It is still noteworthy that a main driving force for the second protonation in the acid catalysed path is provided by the high activation, by the effective π-electron releaser binding metal centre, of the allene ligand towards electrophilic attack. However, this protonation can only occur after the first proton addition to the chloride ligand which competes favourably (for the above mentioned reasons) with the allene for the proton.

Acid-independent path. The monoprotonated intermediate should be able to convert into the final η^2-vinyl complex not

Table 4 Selected bond lengths (Å) for the transition states **TS1**, **TS2** and **TS3**

	TS1	TS2	TS3
C(1)–C(2)	1.332	1.376	1.317
C(1)–C(5)	1.717	1.446	1.396
Re–C(1)	2.138	2.121	2.152
Re–C(5)	2.113	2.164	2.231
Re–P(av.)	2.56	2.55	2.54
Re–Cl(13)	2.585	2.584	2.821
C(5)–H(26)	1.489		
C(1)–H(26)	1.161	1.202	
C(2)–H(26)		1.528	
Cl(13)–H(26)			1.456
Re–H(26)			1.946

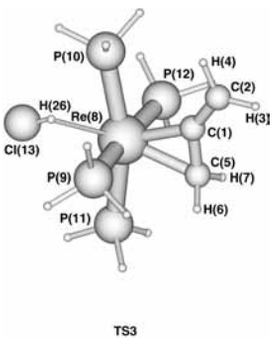

Fig. 4 The transition state for the Cl(13) ⟶ Re proton migration.

only following the dominant acid–base catalysed pathway discussed above, but also by a slower process involving proton shift to the C(2) carbon.

The study of the proton migration from the initial protonated atom [Cl(13) (structure **8**), C(5) (structure **5**) or Re (structures **6** and **7**)] to C(2) indicates that, for these model complexes, the shift cannot occur in a direct way and should involve the intermediate formation of C(1)-protonated structures for the simplified models. However, in the real system the C(1) atom is not expected to be susceptible to protonation (see above) and the present results are thus not fully transferable to the real complexes. The saddle points corresponding to the transition states (TS) for the C(5) ⟶ C(1), C(1) ⟶ C(2) and Cl(13) ⟶ Re proton migration (**TS1**, **TS2** and **TS3**, respectively) were located (Fig. 4 for **TS3**, Table 4). For these transition states, the added proton H(26) is localized between the C(5) and C(1), the C(1) and C(2) or the Cl(13) and Re atoms, and the activation energy for the corresponding proton migrations, calculated as the difference between the energies of the transition state and of the appropriate initial protonated structure, is 56.3, 60.7 and 9.2 kcal mol^{-1}, respectively, reflecting a rather high potential barrier for the first two transformations, but a low one for the Cl(13) ⟶ Re proton shift. This suggests that proton migration from the HCl ligand in **8** occurs *via* the metal to form a hydride intermediate which, by 1,3-hydrogen shift in the real system, would form the final η^2-vinyl product **4**, thus following the order of increasing stability of the complexes involved. This is also consistent with the short distances (2.96 and 2.98 Å) between the hydride proton in the model structures **6** or **7** and the C(2) atom. Nevertheless, the above difficulties encountered by the proton shift to C(2) are in accord with the slower rate of the acid-independent pathway to the η^2-vinyl product in comparison with the faster acid–base catalysed route.

From the considerations discussed in this section and in the previous ones the most favourable mechanistic scheme for the protic conversion of the allene into the η^2-vinyl complex can assume the form shown by Scheme 3.

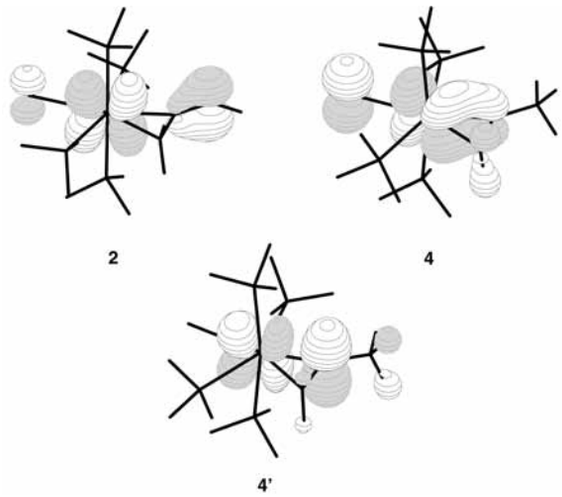

Fig. 5 The HOMOs of the allene (**2**), η^2-vinyl (**4**) and reduced η^2-vinyl (**4′**) complexes.

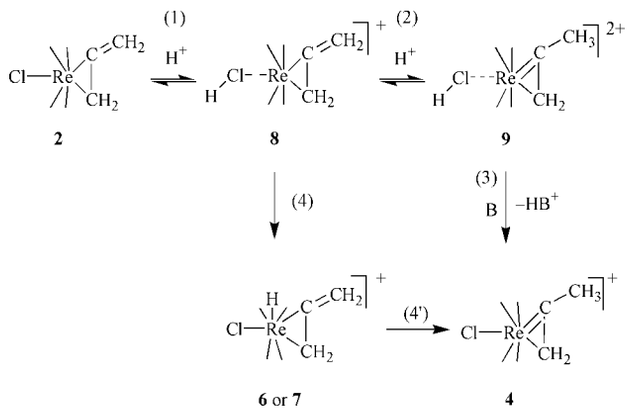

Scheme 3 The most plausible mechanism of protonation of the model complex **2**.

MO analyses of the allene and derived η^2-vinyl complexes and their electrochemical behaviour

Additional information on the nature of the chemical bonds in the initial allene and final η^2-vinyl complexes and the interpretation of some electrochemical results can be obtained by analysis of the composition and distribution of the valence molecular orbitals.

The HOMO of the allene complex **2** (its MO diagram has been deposited as ESI) is represented mainly by a Re(d) orbital which gives antibonding π* combinations with the respective p orbitals of the Cl(13) and C(1) atoms and with participation of the p orbital of the C(2) atom (Fig. 5). It is formed by combination of the HOMO of the $\{ReCl(PH_3)_4\}$ fragment with the occupied π (C(1)–C(2)) orbital of the bending allene and its energy is 2.28 eV higher than that of the allene orbital, but lower than that of the metal fragment by 0.32 eV, in contrast with results of extended Hückel calculations[6b] on a more simplified model. The main contributions to the HOMO of **2** are given by the Re and the C(2) atoms (Mulliken atomic populations of 1.32 and 0.38, respectively), whereas those of the Cl(13) and C(1) atoms are weaker but still significant (0.16 and 0.08). Thus, on the basis of simple frontier orbital concepts,[22] initial protonation at the C(5) atom is not expected (the contribution of the orbitals of this atom to the HOMO is about zero) but the initial protonation at the chloro-atom is acceptable. The higher contribution of a C(2) atomic orbital relatively to C(1) is in accord with extended Hückel results[6b] and is accounted for by participation of the virtual allene π* (C(1)–C(2)) MO in the HOMO of **2** as the π–π* combination with predominant contribution of the occupied allene π (C(1)–C(2)) MO.

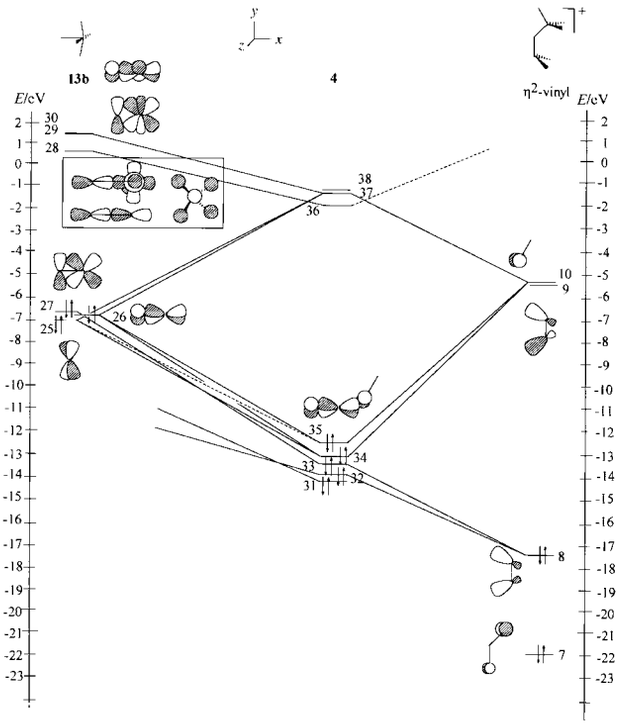

Fig. 6 A molecular orbital diagram for the η^2-vinyl complex **4**.

The second HOMO of complex **2** is mainly localized at the Re atom (the Mulliken population is 1.67) whereas the third HOMO is formed by the virtual allene π* (C(1)–C(5)) MO and the π* (Re–Cl(13)) MO of the $\{ReCl(PH_3)_4\}$ fragment, corresponding to π-electron release from a filled rhenium d orbital to the vacant π* (C(1)–C(5)) orbital of the allene (π-back-bonding component of the Re–allene bond, according to the Dewar–Chatt–Duncanson model,[23] thus accounting for the lengthening of the C(1)–C(5) bond on co-ordination).

For the η^2-vinyl complex **4** the HOMO (Figs. 5 and 6) has contributions from the orbitals of the Re, Cl(13) and C(1) atoms but with a Re(d)–C(1)(p) bonding interaction. In contrast with the allene complex **2**, there is no contribution of the filled π orbitals of the allene in the HOMO. The filled MO next in energy is also formed by Re(d) and C(1)(p) orbitals and is Re–C(1) bonding. Such distinct features of these filled valence MOs of **4**, in comparison with **2**, account well for important differences in the co-ordination of the η^2-vinyl and η^2-allene ligands, the former with a Re=C(1) double bond (carbene) character resulting from an extensive π-electron release from the filled d_{xz} (Re) orbital into the empty p_z (C(1)) orbital, whereas in the latter ligand that bond has a single character and some degree of a destabilizing four-electron interaction occurs (the HOMO in the allene complex results from a great contribution from the filled π (C(1)–(2)) MO of the allene fragment).

The analysis of the MO composition of the allene and vinyl complexes can also allow the rationalization of some features of their electrochemical behaviour. Hence, a considerable destabilization of the filled allene π orbital occurs on co-ordination to form the HOMO (which is metal–allene anti-bonding) in complex **2**, with only a small stabilization of the HOMO of the $\{ReCl(PH_3)_4\}$ fragment. In contrast, a great stabilization of the HOMO takes place in the formation of **4** from the respective fragments $\{ReCl(PH_3)_4\}$ and $C_3H_5^+$ (bonding metal–vinyl combination). Therefore, the HOMO of the allene complex, at a relatively high energy, is greatly destabilized in relation to the HOMO of the vinyl complex, thus accounting for the low value of the oxidation potential of the former complex ($E_{1/2}^{ox} = -0.03$ V *vs.* SCE[11]) and the high anodic shift required for the oxidation of the latter which occurs at $E_{p/2}^{ox} = 1.34$ V.[11]

In accord with these observations, the calculated ionization potential for the vinyl complex is much higher than that for the allene compound. The ionization potential of **2,** obtained on the basis of Koopmans' theorem, is 7.26 eV, and its vertical ionization potential, calculated as the difference of full energies for the equilibrium geometry of **2** and its cationic form with the same geometry (using the unrestricted Hartree–Fock method for both structures without electron correlation correction), is 4.70 eV. The value of 5.60 eV for this ionization potential is obtained by taking into account electron correlation in the MP2 approach. For the vinyl complex **4** the Koopmans ionization potential is 12.30 eV and the vertical ionization potentials, calculated at the HF and MP2 levels, are 9.75 and 10.58 eV.

The vinyl complex can also undergo a single-electron *cathodic reduction* at $E_p^{red} = -1.2$ V to regenerate the parent allene compound, *i.e.* the reduced neutral vinyl complex is unstable and undergoes spontaneous dehydrogenation. For consideration of this process, we calculated the MO distribution (deposited as ESI) of the reduced (neutral) vinyl complex **4′**, assuming that the geometry is retained on reduction. As expected, a change in the order of some valence MOs is observed and the HOMO (Fig. 5) is the singly occupied MO formed on stabilization (by 3.78 eV) of the second LUMO of the initial vinyl complex **4** (Fig. 6). This orbital mainly represents the antibonding combinations of Re(d) with C(1)(p) and therefore filling of this orbital by reduction of the vinyl complex should lead to weakening of the Re–C(1) bond as confirmed by full geometry optimization of the reduced vinyl complex [elongation of the Re–C(1) from 1.935 Å in **4** to 2.148 Å in **4′**]. The added electron is thus localized at the C(1) and Re atoms and homolytic C(2)–H bond cleavage would leave an unpaired electron at the C(2) atom which, by pairing with the former electron, forms the double C(1)–C(2) bond, thus giving the allene complex **2** as the final product.

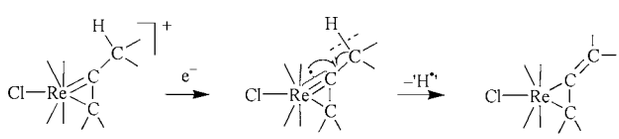

Concluding remarks

Protonation reactions, even when "simply" leading to a product in a quantitative, regiospecific and fast way, can occur *via* complex mechanisms which require detailed kinetic analysis to be established. However, experimental methods are frequently unable to identify short lived intermediates and this work provides an attempt to combine, in a complementary manner, the use of theoretical methods for the identification of such species in order to allow the full establishment of the reaction mechanism.

Such an approach has shown that a ligand, such as chloride, which commonly appears to behave as a mere spectator (or as a *trans*-ligand stabilizer), can in fact play an active and fundamental role in the protonation process, namely constituting the most probable site for the initial proton attack to form the kinetically favoured intermediate (which could be selected among all the possible candidates) that can then convert, *via* further proton attack, into other initially less susceptible sites to protonation or through proton migration (*via* the metal), into thermodynamically more stable products which otherwise would not so readily be formed.

Hence, theoretical methods, combined with chemical, stopped-flow spectrophotometric and electrochemical ones, provide a contribution to the elucidation of proton-addition, proton-shift and dehydrogenation processes of considerable complexity, and to understanding of the structure of the complexes involved and of the bonding of the reactive ligands.

Acknowledgements

This work has been partially supported by the Foundation for Science and Technology (FCT) and the PRAXIS XXI programme (Portugal). M. L. K also acknowledges this programme for the award of a grant (BPD16369/98). We are also indebted to Professor R. Hoffmann for his kind advice and involvement in the early stage of the theoretical investigation of the allene and vinyl complexes.

References

1 See for example: (*a*) S. Niu and M. B. Hall, *Chem. Rev.*, 2000, **100**, 353; (*b*) P. E. M. Siegbahn and M. R. A. Blomberg, *Chem. Rev.*, 2000, **100**, 421; (*c*) M. Torrent, M. Sola and G. Frenking, *Chem. Rev.*, 2000, **100**, 439; (*d*) A. Dedieu, *Chem. Rev.*, 2000, **100**, 543; (*e*) G. Frenking and N. Fröhlich, *Chem. Rev.*, 2000, **100**, 717; (*f*) T. R. Cundari, *Chem. Rev.*, 2000, **100**, 807; (*g*) N. Koga and K. Morokuma, *Chem. Rev.*, 1991, **91**, 823; (*h*) *Reviews in Computation Chemistry*, eds. K. B. Lipkowitz and D. B. Boyd, VCH, New York, 1990–1999, vols. 1–13; (*i*) G. Frenking, C. Bolhme and U. Pidun, *Pauling's Legacy: Modern Modelling of the Chemical Bond. Theoretical and Computational Chemistry*, eds. Z. B. Maksic and W. J. Orville-Thomas, Elsevier, Amsterdam, 1999, vol. 6; (*j*) T. Ziegler, *Chem. Rev.*, 1991, **91**, 651, and references therein.

2 (*a*) E. R. Davidson, K. L. Kunze, F. B. C. Machado and S. J. Chakravorty, *Acc. Chem. Res.*, 1993, **26**, 628; (*b*) T. Ziegler, V. Tschinke and C. Ursenbach, *J. Am. Chem. Soc.*, 1987, **109**, 4825; (*c*) A. W. Ehlers and G. Frenking, *J. Am. Chem. Soc.*, 1994, **116**, 1514; (*d*) A. W. Ehlers and G. Frenking, *Organometallics*, 1995, **14**, 423; (*e*) R. K. Szilagyi and G. Frenking, *Organometallics*, 1997, **16**, 4807; (*f*) V. Jonas and W. Thiel, *J. Chem. Soc.*, *Dalton Trans.*, 1999, 3783; (*g*) V. Jonas and W. Thiel, *J. Chem. Phys.*, 1996, **105**, 3636; (*h*) V. Jonas and W. Thiel, *J. Chem. Phys.*, 1995, **102**, 8474; (*i*) Ch. van Wüllen, *J. Chem. Phys.*, 1996, **105**, 5485; (*j*) D. C. Brower, J. L. Templeton and D. M. P. Mingos, *J. Am. Chem. Soc.*, 1987, **109**, 5203; (*k*) A. J. Lupinetti, S. Fau, G. Frenking and S. H. Strauss, *J. Phys. Chem. A*, 1997, **101**, 9551; (*l*) D. M. P. Mingos, *J. Organomet. Chem.*, 1979, **179**, C29; (*m*) B. E. Bursten, *J. Am. Chem. Soc.*, 1982, **104**, 1299; (*n*) K. G. Kaulton, R. L. De Kock and R. F. Fenske, *J. Am. Chem. Soc.*, 1970, **92**, 515; (*o*) J. C. Green and C. N. Jardine, *J. Chem. Soc.*, *Dalton Trans.*, 1999, 3767; (*p*) G. Hogarth, D. G. Humphrey, N. Kaltsoyannis, W.-S. Kim, M.-Y. V. Lee, T. Norman and S. P. Redmond, *J. Chem. Soc.*, *Dalton Trans.*, 1999, 2705; (*q*) R. Hoffmann, M. M.-L. Chen and D. L. Thorn, *Inorg. Chem.*, 1977, **16**, 503.

3 (*a*) T. E. Taylor and M. B. Hall, *J. Am. Chem. Soc.*, 1984, **106**, 1576; (*b*) E. A. Carter and W. A. Goddard III, *J. Am. Chem. Soc.*, 1986, **108**, 4746; (*c*) J. Ushio, H. Nakatsuji and T. Yonezawa, *J. Am. Chem. Soc.*, 1984, **106**, 5892; (*d*) L. Zhang, M. P. Gamasa, J. Gimeno, A. Galindo, C. Mealli, M. Lanfranchi and A. Tiripicchio, *Organometallics*, 1997, **16**, 4099; (*e*) G. Frenking and U. Pidun, *J. Chem. Soc.*, *Dalton Trans.*, 1997, 1653; (*f*) L. M. Atagi and J. M. Mayer, *Organometallics*, 1994, **13**, 4794; (*g*) P. Hofmann, in *Carbyne Complexes*, eds. H. Fischer, P. Hofmann, F. R. Kreissl, R. R. Schrock, U. Schubert and K. Weiss, VCH Publishers, Weinheim, 1988; (*h*) N. M. Kostic and R. F. Fenske, *Organometallics*, 1982, **1**, 489; (*i*) N. M. Kostić and R. F. Fenske, *Organometallics*, 1982, **1**, 974; (*j*) N. M. Kostić and R. F. Fenske, *J. Am. Chem. Soc.*, 1981, **103**, 4677; (*k*) M. Bamber, G. C. Conole, R. J. Deeth, S. F. T. Froom and M. Green, *J. Chem. Soc.*, *Dalton Trans.*, 1994, 3569; (*l*) R. Stegmann and G. Frenking, *Organometallics*, 1998, **17**, 2089; (*m*) M. L. Buil, O. Eisenstein, M. A. Esteruelas, C. García-Yebra, E. Gutiérrez-Puebla, M. Oliván, E. Oñate, N. Ruiz and M. A. Tajada, *Organometallics*, 1999, **18**, 4949.

4 J. N. Murrell, A. Al-Derzi, G. J. Leigh and M. F. Guest, *J. Chem. Soc.*, *Dalton Trans.*, 1980, 1425; E. M. Shustorovich, G. I. Kagan and G. M. Kagan, *Zh. Struct. Khim.*, 1970, **11**, 108; S. M. Vinogradova, M. G. Kaplunov and Yu. G. Borodko, *Zh. Struct. Khim.*, 1972, **13**, 67; Yu. A. Kruglyak and K. B. Yatzimirski, *Teor. Eksp. Khim.*, 1969, **5**, 308; K. B. Yatzimirski, Yu. P. Nazarenko, Yu. I. Bratushko and Yu. A. Kruglyak, *Teor. Eksp. Khim.*, 1970, **6**, 729; Yu. I. Bratushko, Yu. P. Nazarenko and K. B. Yatzimirski, *Teor. Eksp. Khim.*, 1973, **9**, 13; I. V. Golovanov and V. M. Sobolev, *Teor. Eksp. Khim.*, 1974, **10**, 327; I. V. Golovanov, V. M. Sobolev and M. V. Volkenshtein, *Teor. Eksp. Khim.*, 1976, **12**, 467; I. V. Golovanov, V. M. Sobolev and M. V. Volkenshtein, *Dokl. Akad. Nauk SSSR*, 1974, **218**, 1218; I. M. Treitel, M. T. Flood, R. E. Marsh and H. B. Gray, *J. Am. Chem. Soc.*, 1969, **91**, 6512; R. D. Harcourt, *J. Mol. Struct.*, 1971, **8**, 11; D. L. DuBois and R. Hoffmann, *Nouv. J. Chem.*, 1977, **1**, 479.

5 K. Tatsumi, R. Hoffmann and J. L. Templeton, *Inorg. Chem.*, 1982, **21**, 466; U. Pidun and G. Frenking, *J. Organomet. Chem.*, 1996, **525**, 269; U. Pidun and G. Frenking, *Organometallics*, 1995, **14**, 5325; A. J. Nielson, P. D. W. Boyd, G. R. Clark, T. A. Hunt, J. B. Metson, C. E. F. Rickard and P. Schwerdtfeger, *Polyhedron*, 1992, **11**, 1419; T. Ziegler and A. Rauk, *Inorg. Chem.*, 1979, **18**, 1558; K. Kitaura, S. Sakaki and K. Morokuma, *Inorg. Chem.*, 1981, **20**, 2292; S. Sakaki, K. Kitaura and K. Morokuma, *Inorg. Chem.*, 1982, **21**, 760; C. N. Wilker, R. Hoffmann and O. Eisenstein, *Nouv. J. Chim.*, 1983, **7**, 535; J. Uddin, S. Dapprich, G. Frenking and B. F. Yates, *Organometallics*, 1999, **18**, 457; C. Carfagna, N. Carr, R. J. Deeth, S. J. Dossett, M. Green, M. F. Mahon and C. Vaughan, *J. Chem. Soc.*, *Dalton Trans.*, 1996, 415.

6 (*a*) A. S. Gamble, K. R. Birdwhistell and J. L. Templeton, *J. Am. Chem. Soc.*, 1990, **112**, 1818; (*b*) A. J. L. Pombeiro, D. L. Hughes, R. L. Richards, J. Silvestre and R. Hoffmann, *J. Chem. Soc.*, *Chem. Commun.*, 1986, 1125; (*c*) E. A. Kochetkova and A. F. Shestakov, *Kinet. Katal.*, 1991, **32**, 522; (*d*) C. P. Casey, J. T. Brady, T. M. Boller, F. Weinhold and R. K. Hayashi, *J. Am. Chem. Soc.*, 1998, **120**, 12500.

7 M. F. N. N. Carvalho, A. J. L. Pombeiro, E. G. Bakalbassis and C. A. Tsipis, *J. Organomet. Chem.*, 1989, **371**, C26; E. G. Bakalbassis, C. A. Tsipis and A. J. L. Pombeiro, *J. Organomet. Chem.*, 1991, **408**, 181.

8 J. Silvestre and R. Hoffmann, *Helv. Chim. Acta*, 1985, **68**, 1461.

9 A. DelMedico, S. S. Fielder, A. B. P. Lever and W. J. Pietro, *Inorg. Chem.*, 1995, **34**, 1507; T. Funabiki and T. Yamazaki, *J. Mol. Catal. A: Chem.*, 1999, **150**, 37; S. Bellemin-Laponnaz, J. P. Le Ny and A. Dedieu, *Chem. Eur. J.*, 1999, **5**, 57; Y. Le Mest, C. Inisan, A. Laouénan, M. L'Her, J. Talarmin, M. El Khalifa and J.-Y. Saillard, *J. Am. Chem. Soc.*, 1997, **119**, 6095; P. Fantucci and S. Lolli, *J. Mol. Catal.*, 1993, **82**, 131; S. Niu, L. M. Thomson and M. B. Hall, *J. Am. Chem. Soc.*, 1999, **121**, 4000; J. I. García, V. Martínez-Merino and J. A. Mayoral, *J. Org. Chem.*, 1998, **63**, 2321; S. Strömberg, K. Zetterberg and P. E. M. Siegbahn, *J. Chem. Soc.*, *Dalton Trans.*, 1997, 4147; P. Margl and T. Ziegler, *J. Am. Chem. Soc.*, 1996, **118**, 7337; Y. Han, L. Deng and T. Ziegler, *J. Am. Chem. Soc.*, 1997, **119**, 5939; S. Niu and M. B. Hall, *J. Am. Chem. Soc.*, 1999, **121**, 3992.

10 R. A. Henderson, A. J. L. Pombeiro, R. L. Richards and Y. Wang, *J. Organomet. Chem.*, 1993, **447**, C11.

11 M. A. N. D. A. Lemos and A. J. L. Pombeiro, *J. Organomet. Chem.*, 1988, **356**, C79.

12 L. Szasz, *Pseudopotential Theory of Atoms and Molecules*, Wiley, New York, 1985; M. Krauss and W. J. Stevens, *Annu. Rev. Phys. Chem.*, 1984, **35**, 357.

13 M. W. Schmidt, K. K. Baldridge, J. A. Boatz, S. T. Elbert, M. S. Gordon, J. H. Jensen, S. Koseki, N. Matsunaga, K. A. Nguyen, S. J. Su, T. L. Windus, M. Dupuis and J. A. Montgomery, *J. Comput. Chem.*, 1993, **14**, 1347.

14 C. Møller and M. S. Plesset, *Phys. Rev.*, 1934, **46**, 618; J. S. Binkley and J. A. Pople, *Int. J. Quantum Chem.*, 1975, **9**, 229.

15 D. Andrae, U. Haeussermann, M. Dolg, H. Stoll and H. Preuss, *Theor. Chim. Acta*, 1990, **77**, 123.

16 A. Bergner, M. Dolg, W. Kuechle, H. Stoll and H. Preuss, *Mol. Phys.*, 1993, **80**, 1431.

17 R. Ditchfield, W. J. Hehre and J. A. Pople, *J. Chem. Phys.*, 1971, **54**, 724.

18 D. L. Hughes, A. J. L. Pombeiro, C. J. Pickett and R. L. Richards, *J. Chem. Soc.*, *Chem. Commun.*, 1984, 992.

19 F. H. Allen, O. Kennard, D. G. Watson, L. Brammer, A. G. Orpen and R. Taylor, *J. Chem. Soc.*, *Perkin Trans. 2*, 1987, S1.

20 S. S. P. R. Almeida and A. J. L. Pombeiro, *Organometallics*, 1997, **16**, 4469.

21 T. Al Salih, M. T. Duarte, J. J. R. Fraústo da Silva, A. M. Galvão, M. F. C. Guedes da Silva, P. B. Hitchcock, D. L. Hughes, C. J. Pickett, A. J. L. Pombeiro and R. L. Richards, *J. Chem. Soc.*, *Dalton Trans.*, 1993, 3015; M. F. Meidine, M. A. N. D. A. Lemos, A. J. L. Pombeiro, J. F. Nixon and P. B. Hitchcock, *J. Chem. Soc.*, *Dalton Trans.*, 1998, 3319.

22 K. Fukui, *Theory of Orientation and Stereoselection*, Springer Verlag, Berlin, 1975.

23 M. J. S. Dewar, *Bull. Soc. Chim. Fr.*, 1951, **18**, C71; J. Chatt and L. A. Duncanson, *J. Chem. Soc.*, 1953, 2939.